Surface & Coatings Technology 268 (2015) 85–89

Contents lists available at ScienceDirect

Surface & Coatings Technology

journal homepage: www.elsevier.com/locate/surfcoat

Oxidation performance of cold spray Ti–Al barrier coated γ-TiAl intermetallic substrates

J. Cizek [a,*], O. Man [a], P. Roupcova [a], K. Loke [b], I. Dlouhy [a]

[a] Netme Centre, Institute of Materials Science and Engineering, Brno University of Technology, Czech Republic
[b] Singapore Technologies — Kinetics, Ltd., Singapore

ARTICLE INFO

Available online 8 December 2014

Keywords:
Cold spray
Oxidation protection
TiAl
Intermetallics
Heat treatment

ABSTRACT

Four blends of Al powder containing different amounts of Ti were deposited onto Ti–46Al–7Nb substrates as oxidation–protection layers using low-pressure cold spray. The coating morphology and chemical composition were assessed. Optimized heat treatment in protective atmosphere was carried out in order to induce formation of intermetallic phases within the deposits. The specimens were then subjected to 950 °C exposure for 100, 250, and 500 h and their oxidation performance was monitored using the gravimetric method.
It was found that the oxidation rate of the coating-protected specimens was substantially reduced (an increase in the weight gain of 1.37 mg·cm^{-2} after 500 h of specimen with Al coating) as compared to their uncoated counterparts (1.21 mg·cm^{-2} after 50 h at 900 °C). The oxidation rates increased with increasing content of Ti in the coatings. Substantial changes of the coating integrity were recorded after the long-term oxidation testing.

1. Introduction

Owing to their favorable properties, near-γ titanium aluminides are used in automotive, aerospace and power generation industries [1]. They offer relatively low density (3.7–3.9 g·cm^{-3}), superior stiffness (175 GPa at 20 °C) and strength (up to 650 MPa), lower thermal expansion coefficient (8.5 × 10^{-6} at 20 °C), good oxidation and creep resistance up to moderately high temperatures and high thermal conductivity.

There are, however, limiting factors influencing their potential use, such as poor hydrogen permeation resistance, reduced crack resistance at temperatures up to 450 °C, high susceptibility to surface quality defects and mainly an insufficient oxidation resistance at temperatures above 750 °C [2–4]. It was shown that a short time exposure to oxidizing atmospheres at 700 °C led to a dramatic deterioration of mechanical properties [5]. As the application temperature ranges for TiAl alloys lie between 700–800 °C, the high-temperature oxidation resistance is a crucial factor determining the performance of the engineering components.

Cold spraying is a surface modification process, whereby protective or function-performing coatings are deposited onto substrates at room to moderate temperatures. Individual particles of the deposited materials are introduced into a supersonic gas flow (He, Ar, compressed air) and are accelerated in a Laval nozzle. Upon hitting the substrate, they undergo plastic deformation, creating a coherent layer of added material [6,7]. As opposed to its high-temperature counterparts, the solid state impact represents the major advantage of the process [8–12].

The current cold spray techniques could be divided into high-pressure and low-pressure systems [13]. Contrary to high-pressure processes, a significant amount of coating porosity generally arises within the low-pressure deposition. Its content could amount up to 30% in thin coatings [13]. In some applications, such pore content might negatively affect the functionality of the coatings. As such, several ways to reduce the total porosity were proposed in the literature:

- the addition of heavier particles into the initial feedstock was shown to trigger the "hammering effect", i.e. closing of internal porosity due to the impact of heavier particles (the effect was observed e.g. by Koivuluoto in [14]).
- improved filling of the intersplat voids was reported by using bimodal powder size distribution (e.g. for warm sprayed Ti coatings in [15]).
- the porosity of cold sprayed coatings could be further reduced via multiple torch passes. The compressive effect of the incoming particles densifies the previously deposited layers.

The objective of the presented study was to improve the oxidation behavior of near-γ TiAl intermetallics by a cold spray deposition of protective Al coatings. The effectiveness of the protection is directly linked to the coating porosity, in particular the presence/absence of interconnected voids potentially exposing the substrate. In order to decrease the coating porosity, the above mentioned densification mechanisms were implemented via Ti powder addition into the Al feedstock. As the influence of Ti content on the porosity was not known, four Al:Ti feedstock ratios were selected for evaluation. Moreover, the addition

* Corresponding author.
E-mail address: cizek@fme.vutbr.cz (J. Cizek).

http://dx.doi.org/10.1016/j.surfcoat.2014.12.004
0257-8972/

of Ti could lead to formation of intermetallic phases in the coatings when heat treated properly. Such formation [16,17] might lead to stabilization or suppression of the oxidation process [18]. To exploit this phenomenon, the coated samples were heat-treated in a protective oxygen-free atmosphere at various temperatures and dwell times. The oxidation performance of the specimens was then evaluated in a high-temperature oxidizing environment. Morphological and chemical changes in the coatings and substrates were further observed after extended exposure times with respect to their uncoated counterparts.

2. Experimental

2.1. Materials

Commercially available Al (14–77 μm, oval morphology, GTV, Germany) and Ti (11–50 μm, angular morphology, HC Starck, Germany) thermal spray powders were used in this study. According to the material datasheets, the powders contained 0.1% (Al) and 0.3% (Ti) oxygen content. No additional phases were detected by X-ray diffraction.

As a substrate material, hot-cast Ti–46Al–7Nb–0.7Cr–0.2Ni–0.1Si alloy was used (Flowserve Corporation, USA). The material exhibited duplex structure with predominantly γ-TiAl lamellar morphology and a presence of fine grains located in-between the lamellar colonies (bright contrast areas in Fig. 1). According to EBSD studies performed by Hasegawa et al. [19,20], the grains are considered as β phase (BCC; as such, the alloy ranks as "near-γ"). In the lamellar γ structure, the EDX analysis revealed a higher Nb content in the bright-appearing lamellae (preferably oriented Nb-rich lamellae in Al-richer matrix). The average micro-hardness of the substrate material was specified as 335 HV 0.3.

2.2. Coating deposition

Substrate specimens were wire-cut in the dimensions of 3.2 × 4.2 × 75 mm. Given the high propensity of TiAl-based intermetallics to surface cracking, standard mechanical preparation procedure of the samples could not be employed. Instead, electro-polishing of the exposed surfaces was applied in a solution of nitric acid, perchloric acid, and ethyl alcohol. No grit blasting prior to the coating deposition was used.

Four blends of the Al powder containing 0, 5, 15, and 30 wt.% Ti were deposited. For the deposition, ITAM RAS low-pressure cold spray system (Singapore Technologies-Kinetics, Singapore) was used at 1.64 MPa pressure (the parameters used for deposition are shown in Table 1).

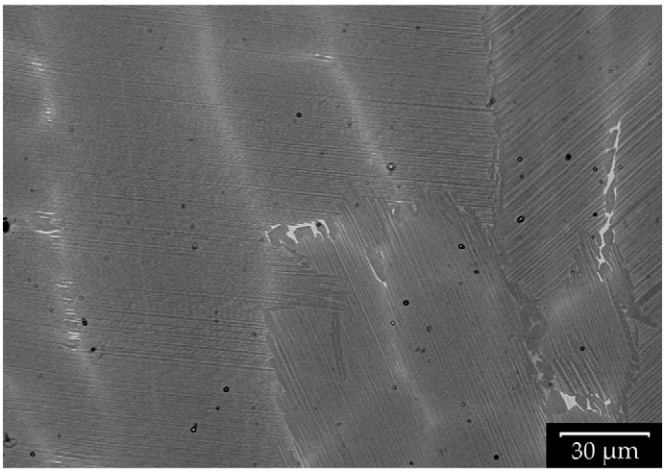

Fig. 1. Morphology of the substrate material (SEM, backscattered electrons). The duplex structure consists of γ-TiAl lamellar colonies and precipitated β phase (bright contrast areas).

The used compressed air was heated to 300 °C, well below the melting temperatures of both powders. Using a dedicated holder, 18 samples were sprayed simultaneously per each set. All four major faces of the specimens were covered, with the target coating thickness set to reach 700–800 μm. The excessive thickness of the coatings was selected to meet two objectives: 1) to provide Al reservoir for the passivation process via intensified diffusion into the substrate and 2) to seal any interconnected porosity/void chains that might expose the underlying substrate surface via peening effect of multiple nozzle passes described in the Introduction section.

2.3. Thermal pre-treatment and isothermal loading experiments

Inert atmosphere heat treatment was carried out after the deposition. For the treatment, temperatures of 420 °C–580 °C were used for 5 h [17]. Inside the furnace, the samples were placed onto a ceramic holder to prevent contamination and a continuous flow of argon was maintained at 0.60 $l \cdot min^{-1}$ to preserve the inert character of the environment during the treatment. Such treatment aimed at formation of (preferably Al-rich) intermetallic phases in the coatings. Concurrently, diffusion of Al and Ti atoms into the substrate was expected to aid the oxidizing resistance via passivation layer formation during the subsequent high temperature testing [21,22].

Following the pre-treatment, the specimens were subjected to a 950 °C long-term exposure in air to study their oxidation performance. Given the application temperature range of the substrate material (700–800 °C), the increased temperature was selected to intensify the oxidation process, thereby reducing the required testing times. Due to the dimensions of the samples, standard thermogravimetry analysis (TGA) method could not be implemented to assess the oxidation process. The samples conventionally used for TGA analyses would require additional cutting of the coated specimens, leading to exposure of faces of the underlying substrate. In such case, the ratio of uncoated and coated faces would be altered significantly. Therefore, non-continuous weighing of the whole samples using a precision balance (resolution 0.1 mg) was carried out instead and the weight gain over time per unit of surface area was calculated at given time intervals. To emphasize the oxidation process impact and facilitate the weight gain detection, exposure times of 100, 250, and 500 h were used.

3. Results and discussion

3.1. Coating properties

The Al–Ti coatings were deposited with an average thickness of (750 ± 90) μm. The cross-section of the produced coatings is shown in Fig. 2. The respective Ti content was specified as 0, 5.4, 13.4, and 32.8 wt.% by image analysis method, i.e. the feedstock Al:Ti ratio was retained in the coatings. The inherent porosity of the produced coatings reached > 5.9%. Such level of porosity is a consequence of the low deposition gas pressures of the device used and was also observed elsewhere [16]. No phase changes or oxidation as compared to the feedstock materials were detected in the coatings by energy-dispersive X-ray spectroscopy (EDX) and X-ray diffraction (XRD) methods.

Table 1
Cold spray parameters for deposition of coatings.

Spray medium	Compressed air
Nozzle material	Stainless steel
Work gas pressure	1.52 MPa
Carrier gas pressure	1.64 MPa
Heating current	260 A
Feedrate frequency	70 Hz
Robot speed	60 $mm \cdot s^{-1}$
Robot arm passes	5
Spray distance	12 mm

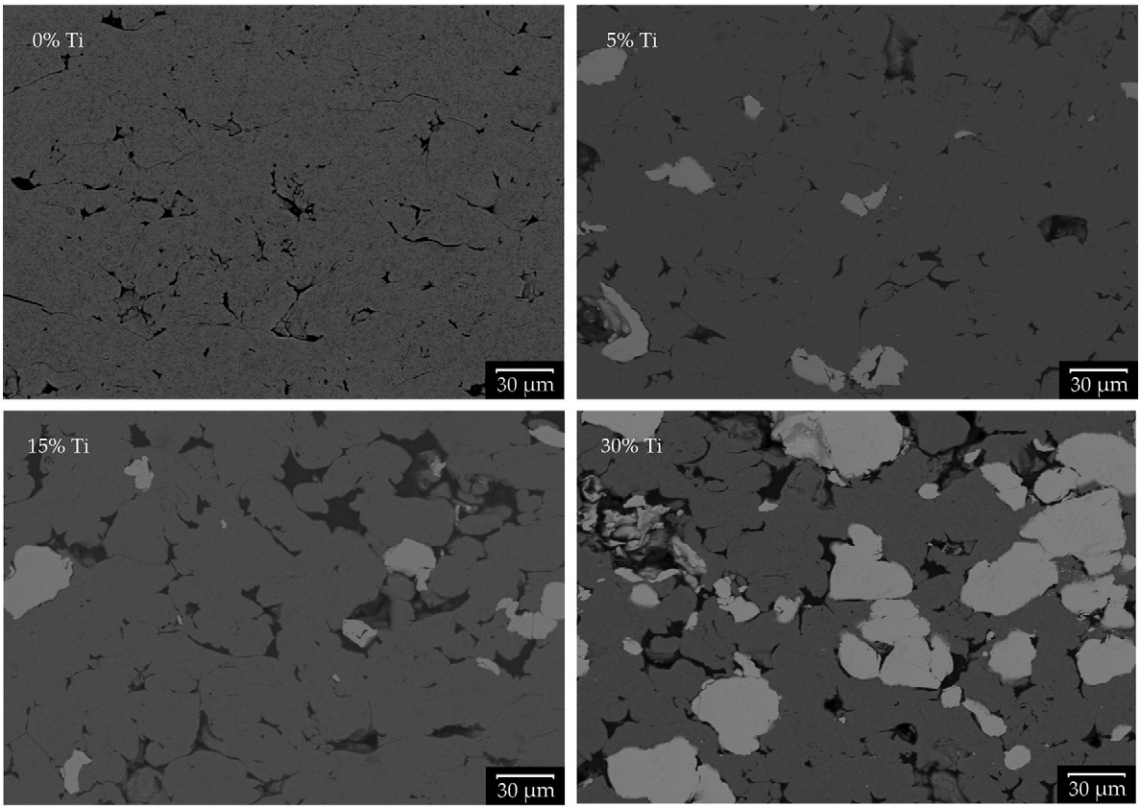

Fig. 2. As-deposited Al–Ti coatings morphology (SEM, backscattered electrons).

3.2. Inert atmosphere pre-treatment

Morphological and composition investigations of the inert atmosphere heat treated specimens allowed determining optimal treatment condition. The treatment at 400 °C did not induce any apparent changes in the samples. As no intermetallic phases were formed in the coatings and no significant Al diffusion into the substrate was observed, the subsequent high temperature testing at 950 °C could have caused melting of the aluminum splats. Such process would invalidate the results of the weight gain measurement and, furthermore, fully expose the underlying substrate.

A formation of pronounced Kirkendall porosity [23] in the coatings was recorded for the treatment carried out at 580 °C. Such response was observed at temperatures lower than those indicated in the studies of Kong and co-workers ([18], 630 °C, argon flow) and Sienkiewicz et al. ([24], 600 °C, evacuated containers). The presence of Kirkendall voids in the material could create open porosity channels in the coatings, effectively exposing the underlying substrates. As a consequence, the results of the subsequent oxidation evaluation could be negatively affected. This temperature therefore could not be used.

The treatment at 500 °C exhibited formation of Al_3Ti intermetallic phase in the Ti splats (Fig. 3). The preferential formation of the Al_3Ti phase was also observed in [18,24] and could be explained by the difference in the mutual Ti/Al solubility limits at temperatures around 600 °C and the Gibbs formation energy of the compound [25,26]. Simultaneously, diffusion of the Al atoms into the substrate was observed, leading to a formation of Al_3Ti in its uppermost layers. The diffusion of Al atoms into the substrate occurred preferably along the Al-rich channels in-between the Nb-rich lamellae in the γ structure, as indicated by the diffusion front line in the magnified view in Fig. 3. After 5 h treatment,

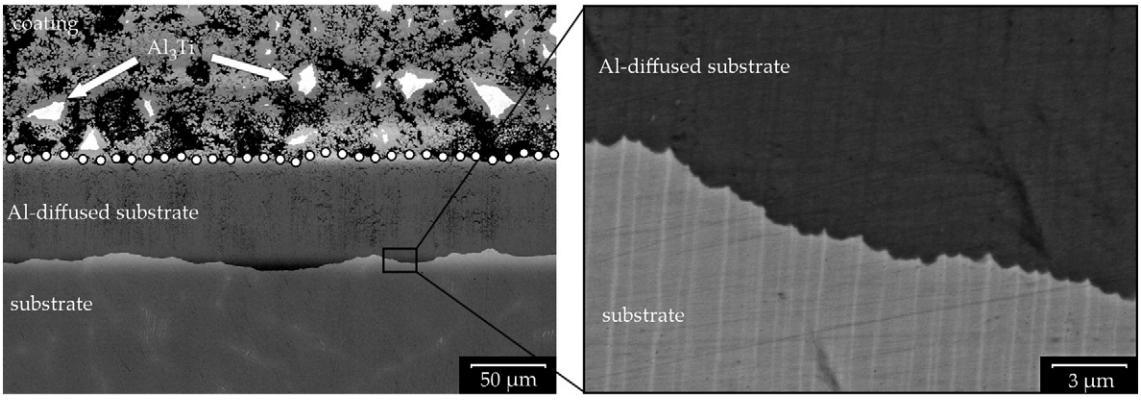

Fig. 3. Changes in coated samples after inert atmosphere pre-treatment at 500 °C (SEM, backscattered electrons). Dots indicate the coating-substrate interface. Formation of Al_3Ti intermetallics is observed in Ti splats in the coatings. Al diffusion from the coatings into the substrates propagated preferably along the Nb-rich lamellae (inset).

the depth of the Al diffusion into the substrate reached approximately 150 μm, triggering a minor coarsening of the lamellar structure. No significant diffusion of Ti atoms into the substrate was observed. No oxidation of the materials was recorded as no oxygen-based phases were detected by XRD method. Based on the results, it was decided to carry out all pre-treatments at 500 °C/5 h.

3.3. High-temperature oxidation

Isothermal exposure of the samples at 950 °C was then carried out. The three coated sets were tested for 100, 250 and 500 h. As a benchmark, an uncoated reference set from previous study [27] was used, tested at 900 °C. Under such conditions, the reference set exhibited an increase in the weight gain of 1.21 $mg \cdot cm^{-2}$ after only 50 h exposure and the rate further increased beyond sample structure limits after >150 h [27].

The oxidation rates of the substrates (Fig. 4) were substantially reduced by the deposition of the coatings. Given the measured differences in oxide layer growth for the respective sets at different holding times, it could be assumed that the major factors influencing the oxide scale formation are manifested in the early stages of the treatment already (100 h exposure time) and the oxidation rate exhibits a saturation. The best performance was observed for the coating containing Al splats only (1.37 $mg \cdot cm^{-2}$ after 500 h exposure). Despite the expected beneficial effects (provided in Introduction and e.g. [18]), the increasing content of Ti splats in the coatings adversely affected the oxidation behavior of the samples (Fig. 4). Given the TiAl oxidation mechanisms (described e.g. in [21,22]), the formation of passivation Al_2O_3 layer at the substrate surface was inhibited by the formation of TiO2 layer. As such, the oxidation process was probably driven by a reduced diffusion of Al atoms through the layers. This led to a retardation of Al_2O_3 layer build-up, resulting in inferior oxidation resistance of the samples. Further to that, the detrimental effect of Ti addition could have been amplified by a sooner depletion of Al atoms in the diffused substrate layer (Fig. 3) due to a formation of Al_3Ti intermetallics in the coatings.

Using SEM and EDX techniques, it was confirmed that the enhanced diffusion in the coatings resulted into a full conversion of remaining Ti particles into Al_3Ti and Al_5Ti_3 intermetallics and the structure of the particles and the porosity changed substantially (Fig. 5, left). Two major oxides, namely Al_2O_3, TiO_2, were detected in the coatings: TiO2 was detected in the inner shells of the particles, while the aluminum oxides surrounded the particles, creating a layer approximately 1 μm thick. A disintegration of the outer coating surfaces structure was observed, an attribute manifested by a spallation of burn-off scales of the material.

A presence of various stoichiometry intermetallic phases was detected in the substrates. The Al-diffusion front reached up to 500 μm into the substrate. In this area, the material consisted mainly of Al_2Ti phase (Fig. 5, right; observed also in [17]). Approximately 10–20 μm from the front, pearl-like Nb-rich crystallites nucleated from the Al_2Ti phase (bright areas in Fig. 5, right). Based on EDX mapping of the region, it could be assumed that the crystallites are formed as a consequence of the interaction of the diffusing Al atoms and the Nb-rich γ lamellar structure of the original as-cast material. Rather than $AlNb_3$ intermetallic phase, the crystallites are most likely formed by solid solution of Al in BCC Nb. Due to the gradient of diffused Al content, the formed intermetallics further changed the stoichiometry towards the substrate-coating interface ($Al_2Ti \rightarrow Al_2Ti + Al_3Ti \rightarrow Al_3Ti \rightarrow Al + Al_3Ti$). Due to these changes, the lamellar structure of the substrate was not retained after the oxidation test; the Nb-rich lamellae diffused into the Al enriched matrix.

4. Conclusions

The current study showed that the oxidation rate of the sensitive γ-TiAl-based intermetallic materials could be substantially hindered by a cold spray deposition of protective layers. Heat treatment in inert atmosphere induced diffusion-driven formation of Al_3Ti intermetallic phase in the coatings and enabled saturation of the substrate material with faster diffusing Al atoms. Upon long-term isothermal heat treatment in an oxidizing atmosphere, the weight increment due to oxide formation was monitored and the morphology and composition changes were observed. From the results it could be concluded that:

- optimal pre-treatment temperature of the Ti-containing Al coatings is ~500 °C in order to induce intermetallic phase formation, but below 580 °C to avoid formation of Kirkendall porosity.
- isothermal exposure to oxidizing environment at 950 °C deteriorates the structure of both the coatings (partial spallation) and the substrate after 100 h exposure already; the initial lamellar structure of the cast

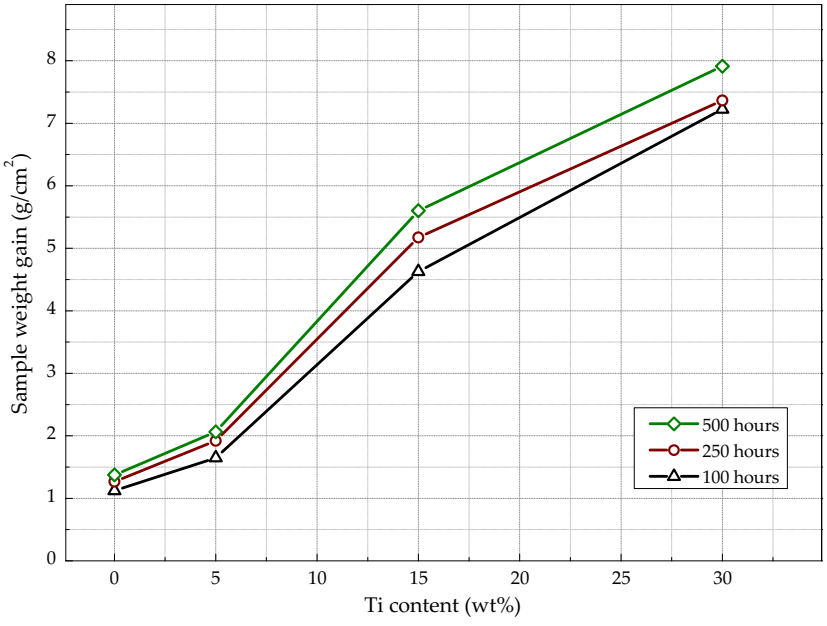

Fig. 4. Influence of Ti content in the coatings on weight gain of samples during isothermal exposure.

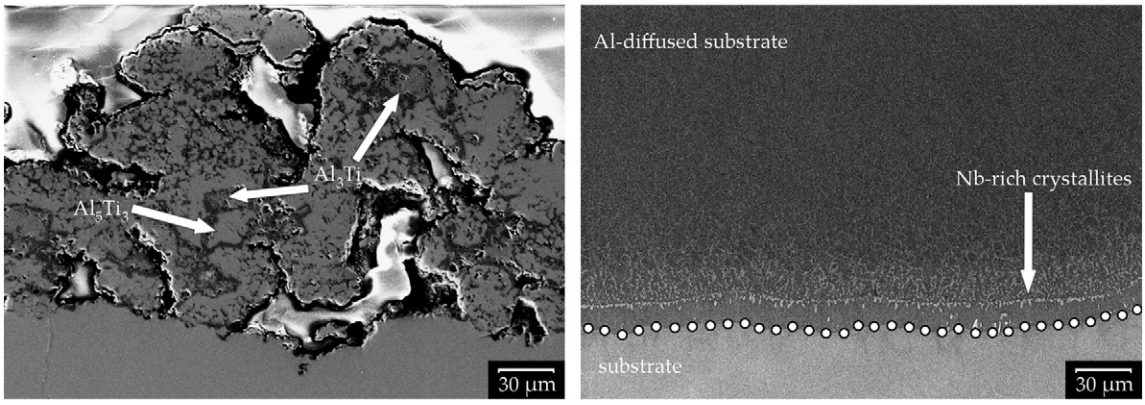

Fig. 5. Morphology of the Ti-containing Al coating (left) and substrate (right) after 500 h oxidizing isothermal loading at 950 °C (SEM, backscattered electrons). Full conversion of Ti particles into Al_5Ti_3, Al_3Ti intermetallics was observed in the coatings. The Al diffusion front reached up to 500 μm in the substrates, predominantly leading to a formation of Al_2Ti phase in the diffused zone (dark gray area; dots indicate the Al-diffusion front).

alloy is not retained probably due to the diffusion of Al into the substrate and a formation of solid solution of Al in Nb.
- the oxidation rate of the specimens is significantly reduced by a deposition of cold sprayed Al + Ti coatings, probably due to the easier formation of Al_2O_3 scale due to the added Al.
- an increase in Ti content in the coatings adversely affects the oxidation resistance, probably due to an inhibition of Al_2O_3 passivation layer formation and earlier depletion of Al atoms in the substrate via formation of Al_3Ti phases in the coatings.

Acknowledgments

The authors would like to express their gratitude to Mrs. Drahomira Janova from Institute of Materials Science and Engineering, Brno University of Technology for the microstructure and EDX investigations.

The Project has been funded from the SoMoPro Programme (Grant no. 229603). Research leading to these results has received a financial contribution from the European Community within the Seventh Framework Programme (FP/2007–2013) under Grant Agreement No. 229603. The research is also co-financed by the South Moravian Region. Support of Czech Science Foundation project GACR 13-35890S is further acknowledged.

References

[1] H. Clemens, H. Kestler, Adv. Eng. Mater. 2 (9) (2000) 551–570.
[2] X.J. Xu, L.H. Xu, J.P. Lin, Y.P. Wang, Z. Lin, G.L. Chen, Intermetallics 13 (3–4) (2005) 337–341.
[3] D. Shechtman, M.J. Blackburn, H.A. Lipsitt, Metall. Trans. 5 (6) (1974) 1373–1381.
[4] H.A. Lipsitt, D. Shechtman, R.E. Schafrik, Metall. Trans. 6 (6) (1975) 1991–1996.
[5] M. Thomas, O. Berteaux, F. Popoff, M.P. Bacos, A. Morel, Intermetallics 14 (10–11) (2006) 1143–1150.
[6] T. Schmidt, H. Assadi, F. Gärtner, H. Richter, T. Stoltenhoff, H. Kreye, T. Klassen, J. Therm. Spray Technol. 18 (5–6) (2009) 794–808.
[7] J. Cizek, O. Kovarik, J. Siegl, K.A. Khor, I. Dlouhy, Surf. Coat. Technol. 217 (2013) 23–33.
[8] P. Fauchais, J. Phys. D. Appl. Phys. 37 (9) (2004) R86–R108.
[9] J. Cizek, K.A. Khor, I. Dlouhy, J. Therm. Spray Technol. 22 (8) (2013) 1320–1327.
[10] P. Fauchais, M. Fukumoto, A. Vardelle, M. Vardelle, J. Therm. Spray Technol. 13 (3) (2004) 337–360.
[11] R. Musalek, O. Kovarik, T. Skiba, P. Hausild, M. Karlik, J. Colmenares-Angulo, Intermetallics 18 (7) (2010) 1415–1418.
[12] J. Cizek, K.A. Khor, Surf. Coat. Technol. 206 (8–9) (2012) 2181–2191.
[13] A. Papyrin, V. Kosarev, S. Klinkov, A. Alkimov, V. Fomin, Cold Spray Technology, Elsevier, 2007.
[14] H. Koivuluoto, Microstructural Characteristics and Corrosion Properties of Cold-sprayed Coatings(PhD thesis) Tampere University of Technology, 2010.
[15] J. Kawakita, M. Watanabe, S. Kuroda, H. Katanoda, Proc. International Thermal Spray Conference, DVS-ASM, 2007, pp. 43–47.
[16] T. Novoselova, P. Fox, R. Morgan, W. O'Neill, Surf. Coat. Technol. 200 (8) (2006) 2775–2783.
[17] T. Novoselova, S. Celotto, R. Morgan, P. Fox, W. O'Neill, J. Alloys Compd. 436 (1–2) (2007) 69–77.
[18] L.Y. Kong, L. Shen, B. Lu, R. Yang, X.Y. Cui, T.F. Li, T.Y. Xiong, J. Therm. Spray Technol. 19 (6) (2010) 1206–1210.
[19] M. Hasegawa, T. Nomura, H. Haga, I. Dlouhy, H. Fukutomi, in: B. Strnadel (Ed.), Proceedings of the grant workshop on New Methods of Damage and Failure Analysis of Structural Parts, VSB-TU, Ostrava, 2012, pp. 185–192.
[20] M. Hasegawa, T. Nomura, H. Haga, I. Dlouhy, H. Fukutomi, Int. J. Mater. Res. 105 (11) (2014) 1075–1083.
[21] I.C.I. Okafor, R.G. Reddy, JOM 51 (6) (1999) 35–39.
[22] M. Schmiedgen, P.C.J. Graat, B. Baretsky, E.J. Mittemeijer, Thin Solid Films 415 (1–2) (2002) 114–122.
[23] A.D. Smigelskas, E.O. Kirkendall, Trans. AIME 171 (1947) 130–142.
[24] J. Sienkiewicz, S. Kuroda, R.M. Molak, H. Murakami, H. Araki, S. Takamori, K.J. Kurzydłowski, Intermetallics 49 (2014) 57–64.
[25] L. Xu, Y.Y. Cui, Y.L. Hao, R. Yang, Mater. Sci. Eng. A 435–436 (2006) 638–647.
[26] U.R. Kattner, J.C. Lin, Y.A. Chang, Metall. Trans. A 23 (8) (1992) 2081–2090.
[27] P. Fukatkova, Embrittlement of TiAl intermetallics induced by surface oxidation(Master's thesis) Brno University of Technology, 2010.